THE JOURNAL OF BIOLOGICAL CHEMISTRY
Vol. 280, No. 16, Issue of April 22, pp. 16410–16416, 2005
Printed in U.S.A.

Membrane Topology Mapping of Vitamin K Epoxide Reductase by *in Vitro* Translation/Cotranslocation*

Received for publication, January 21, 2005, and in revised form, February 15, 2005
Published, JBC Papers in Press, February 16, 2005, DOI 10.1074/jbc.M500765200

Jian-Ke Tie‡, Christopher Nicchitta§, Gunnar von Heijne¶, and Darrel W. Stafford‡**

From the ‡Department of Biology, University of North Carolina at Chapel Hill, Chapel Hill, North Carolina 27599, §Department of Cell Biology, Duke University, Durham, North Carolina 27710, and ¶Department of Biochemistry and Biophysics, Stockholm University, SE-10691 Stockholm, Sweden

Vitamin K epoxide reductase (VKOR) catalyzes the conversion of vitamin K 2,3-epoxide into vitamin K in the vitamin K redox cycle. Recently, the gene encoding the catalytic subunit of VKOR was identified as a 163-amino acid integral membrane protein. In this study we report the experimentally derived membrane topology of VKOR. Our results show that four hydrophobic regions predicted as the potential transmembrane domains in VKOR can individually insert across the endoplasmic reticulum membrane *in vitro*. However, in the intact enzyme there are only three transmembrane domains, residues 10–29, 101–123, and 127–149, and membrane-integration of residues 75–97 appears to be suppressed by the surrounding sequence. Results of *N*-linked glycosylation-tagged full-length VKOR shows that the N terminus of VKOR is located in the endoplasmic reticulum lumen, and the C terminus is located in the cytoplasm. Further evidence for this topological model of VKOR was obtained with freshly prepared intact microsomes from insect cells expressing HPC4-tagged full-length VKOR. In these experiments an HPC4 tag at the N terminus was protected from proteinase K digestion, whereas an HPC4 tag at the C terminus was susceptible. Altogether, our results suggest that VKOR is a type III membrane protein with three transmembrane domains, which agrees well with the prediction by the topology prediction program TMHMM.

The K vitamins, phylloquinone (K1), menaquinones (K2), and menadione (K3), are a family of structurally similar, fat-soluble, 2-methyl-1,4-naphthoquinones. The main function of vitamin K is to act as a co-factor for the γ-glutamyl carboxylase that catalyzes the post-translational carboxylation of specific glutamic acid to γ-carboxyglutamic acid (Gla)[1] of variety of vitamin K-dependent proteins (1). Members of the vitamin K-dependent protein family include coagulation factors (factor II, VII, IX, X) as well as several other proteins that function in bone metabolism (2) and signal transduction (3). Concomitant with γ-glutamyl carboxylation, the reduced form of vitamin K (vitamin K hydroquinone) is converted to vitamin K 2,3-epoxide, which must be converted back to vitamin K hydroquinone for the reaction to continue because of limited vitamin K amounts *in vivo* (4). This cyclic conversion of vitamin K establishes a redox cycle known as the vitamin K cycle (5).

VKOR is responsible for the conversion of vitamin K 2,3-epoxide into vitamin K and is highly sensitive to inhibition by coumarin drugs, such as *R*,*S*-warfarin (4-hydroxy-3-(3-oxo-1-phenylbutyl-coumarin)), the most commonly prescribed oral anticoagulant. Warfarin inhibition of VKOR reduces the availability of reduced vitamin K, which reduces the rate of carboxylation and leads to partially carboxylated, inactive vitamin K-dependent proteins. Since its discovery in 1970 (6), numerous futile attempts to purify the enzyme were reported (7–11). Attempts to understand the mechanism underlying warfarin-sensitive vitamin K epoxide reduction have been somewhat more successful (8, 12–15). Recently, the gene encoding VKOR was identified independently by our laboratory (16) and that of Johannes Oldenburg (17). The enzyme was designated VKOR by us and VKORC1 by Oldenburg and co-workers, who assume that there is another sub-unit still to be identified (either view may be correct). VKOR is a 163-amino acid integral membrane protein with a mass of 18.2 kDa.

To understand the structure/function relationships that define VKOR activity, it is necessary to understand its membrane topology, *i.e.* its specific number of TM segments and their location relative to the cytoplasm or endoplasmic reticulum. Several computer programs to predict the topology of membrane proteins are available (18–21). If the location of one of the termini is known, the best current program correctly predicts the topology of 65–70% of those membrane proteins with known crystal structure (20). The reliability of a given topology prediction is increased if the predictions from a number of different programs agree (19, 20). Moreover, using C-terminal reporter fusions, experimental examination of the topology is reliable (22).

In this study, we report an experimental determination of the membrane topology of VKOR. We first determined the topology of VKOR using multiple prediction programs. These predictions were then tested by *in vitro* translation/cotranslocation of a series of VKOR truncations containing an *N*-linked glycosylation reporter tag. Our results suggest that VKOR is a type III membrane protein with three transmembrane domains. The N terminus of VKOR resides in the lumen of the endoplasmic reticulum, and the C terminus resides in the cytoplasm. The N-terminal domain of VKOR, like many type III membrane proteins, is relatively short, which facilitates its transfer into the lumen (23). The main features of our *in vitro* experiments were confirmed by experiments with microsomes derived from insect cells expressing full-length VKOR.

* This work was supported by National Institutes of Health Grant HL48318 (to D. W. S.). The costs of publication of this article were defrayed in part by the payment of page charges. This article must therefore be hereby marked "*advertisement*" in accordance with 18 U.S.C. Section 1734 solely to indicate this fact.

** To whom correspondence should be addressed. Tel.: 919-962-0597; Fax: 919-962-9266; E-mail: dws@E-mail.unc.edu.

[1] The abbreviations used are: Gla, γ-carboxyglutamic acid; VKOR, vitamin K epoxide reductase; VKORC1, vitamin K epoxide reductase complex subunit 1; TM, transmembrane; HPC4, peptide epitope comprising residues; EDQVDPRLIDGK, ER endoplasmic reticulum; RM, canine rough microsomes; MES, 2-(*N*-morpholino)ethanesulfonic acid, hemisodium salt; CHAPS, (3-[(3-cholamidopropyl)di-methylammonio]-1-propane sulfonate); Endo H, endoglycosidase H; PVDF, polyvinylidene difluoride.

EXPERIMENTAL PROCEDURES

Materials—All oligonucleotide primers, the NuPAGE pre-cast gel, and the insect cell expression vector pVL1392 were from Invitrogen. The *in vitro* translation vector pSPUTK was obtained from Stratagene (San Diego, CA). The SP6 mMESSAGE mMACHINE capped mRNA transcription kit and MEGAClear RNA purification kit were obtained from Ambion (Austin, TX). Rabbit reticulocyte lysate, amino acid master mixture, proteinase K, and ribonuclease inhibitor were obtained from Promega (Madison, WI). [^{35}S]Methionine, [^{35}S]cysteine, and the enhanced chemiluminescence Western blotting detection reagents were from Amersham Biosciences. MES, HEPES, CHAPS, and phenylmethylsulfonyl fluoride were from Sigma. BacVector-3000 DNA kit was from Novagen (Madison, WI). *Taq* polymerase and Endo H were from Roche Applied Science. Trans-Blot transfer medium PVDF membrane (0.2 μm) and biotinylated protein size markers were from Bio-Rad. All the restriction endonucleases and T4 DNA ligase were from New England BioLabs (Beverly, MA). Horseradish peroxidase-conjugated secondary antibody was from Jackson Laboratories (West Grove, PA). Dog pancreatic microsomal membranes were prepared as described (24).

Construction of Full-length VKOR Fusions with the NST Reporter Tag at the N or C Terminus—The gene encoding VKOR was amplified by PCR using pVL1392-VKOR (16) as the template. A 5′-NcoI site and 3′-PstI site was introduced into the PCR fragment, and the PCR product was cloned into the *in vitro* translation vector pSPUTK by NcoI/PstI to yield pSPUTK-VKOR. The N-terminal glycosylation acceptor tag with the amino acid sequence of MGG**NST**GGSGGSGGSG was obtained by annealing the oligonucleotides 5′-CATGGGTGGGAACAGCACCGGTGGGAGCGGGGGCAGCGGGGGCAGCGG-3′ and 5′-CATGCCGCTGCCCCCGCTGCCCCCGCTCCCACCGGTGCTGTTCCCACC-3′ followed by ligation to NcoI-digested pSPUTK-VKOR. Joining the vector and the insert by ligation destroys the NcoI site at the 3′ end of the insert. This plasmid was named pSPUTK-NST-VKOR. A C-terminal glycosylation acceptor tag with the amino acid sequence of SGGSGGS**NST**GGSG was obtained by annealing the oligonucleotides 5′-AAGCGGGGGCAGCGGTGGGAGCAACAGCACCGGGGGTAGCGGTCTGCA-3′ and 5′-GACCGCTACCCCCGGTGCTGTTGCTCCCACCGCTGCCCCCGCTTTGCA-3′ followed by ligation to PstI-digested pSPUTK-VKOR. In this case ligation of the PstI-cleaved pSPUTK-VKOR to the insert results in the destruction of the PstI site at the 5′ end of the insert. This plasmid is named pSPUTK-VKOR-NST. A dimer C-terminal glycosylation tag was engineered by first ligating the insert itself and then ligating the product to PstI-digested pSPUTK-VKOR plasmid to yield pSPUTK-VKOR-NST$_2$.

Construction of VKOR Truncations with NST Reporter Tag at the N Terminus—Site-directed mutagenesis was performed to remove the endogenous BamHI site (without affecting the amino acid sequence) at 365 nucleotides of the VKOR cDNA from pSPUTK-NST-VKOR. The resulting plasmid was used as the PCR template to generate various C-terminal truncations of VKOR. A sense oligonucleotide comprising a NcoI site and part of the NST tag-coding sequence was used as 5′ primer for all the PCR reactions. Oligonucleotides containing a BamHI site and various antisense sequences corresponding to the C terminus of the predicted TM domains were used as 3′ primers for the PCR reaction. PCR-amplified fragments containing each of the predicted TM domains and the N-terminal glycosylation reporter tag were cloned into the NcoI/BamHI-cleaved pSPUTK vector.

Construction of VKOR Truncations with NST Reporter Tag at the C Terminus—The C-terminal glycosylation acceptor tag with the sequence of SGGSGGS**NST**GGSG was amplified by PCR using the above pSPUTK-VKOR-NST plasmid as template. A 5′-BamHI site and a 3′-EcoRI site were introduced into the PCR fragment, and the resulting PCR product was cloned to pSPUTK by BamHI/EcoRI to yield pSPUTK-NST. Various VKOR truncations (containing each of the predicted TM segments) were then amplified by PCR from the pSPUKT-NST-VKOR plasmid with the deleted endogenous BamHI site. The 5′ primer encoding the start sequence of VKOR includes a NcoI site. All the 3′ primers were the same as above. PCR products were cloned into NcoI/BamHI-cleaved pSPUTK-NST to yield different VKOR truncations with the glycosylation reporter tag at the C terminus. The 3′-BamHI (GGATCC) site introduced two amino acid residues (glycine and serine) between the VKOR truncations and the NST tag. Construct 1–74/98–130-NST was obtained by connecting the PCR fragment of 1–74 and 98–130. Fragment 1–74 was amplified by using the above 5′ primer and a 3′ primer containing part of the antisense sequence of VKOR ending at amino acid residue 74 with a XbaI site. Fragment 98–130 was amplified by a 5′ primer containing a XbaI site with part of the sense coding sequence of VKOR starting from residue 98 and the above 3′ primer used for VKOR truncation 1–130. The two obtained PCR fragments were ligated simultaneously with NcoI/BamHI-cleaved pSPUTK-NST vector to yield the construct of pSPUTK-NST-1–74/98–130.

A C-terminal glycosylation tag with a sequence of **NST**GGGS, which does not contain the flexible extension linker, was fused to the VKOR truncation of 1–130 by PCR to yield pSPUTK-1–130-NST′. The 5′ primer used is the same as above, and the 3′ primer contains part of the C-terminal antisense sequence of 1–130 VKOR truncation and the antisense sequence of the tag with a BamHI site. The PCR product was cloned to pSPUTK by NcoI/BamHI. All the constructs used for *in vitro* transcription/translation are shown in Fig. 2.

Construction of the Full-length VKOR Fusions with HPC4 Tag at the N or C Terminus in Insect Cell Expression Vector—A 12-amino acid peptide (EDQVDPRLIDGK) of HPC4 epitope (25) was introduced to either the N or C terminus of full-length VKOR. The HPC4-tagged VKOR cDNA was subcloned into the EcoRI site of the insect cell expression vector of pVL1392. The nucleotide sequences of all the constructs were confirmed by the DNA sequencing facility at the University of North Carolina at Chapel Hill.

In Vitro Transcription and Translation/Cotranslocation—Before *in vitro* transcription the recombinant pSPUTK vectors were linearized at the BamHI site immediately 3′ to the C terminus of all the N-terminal NST-tagged VKOR truncation fusions or at the EcoRI site immediately 3′ to the C terminus of all the C-terminal NST-tagged VKOR truncation fusions. Capped mRNA was synthesized by SP6 RNA polymerase and purified by MEGAClear RNA purification kit according to the manufacturer's instructions. The transcription reaction was incubated at 37 °C for at least 5 h to increase the yield of mRNA.

In vitro translations using rabbit reticulocyte lysate, and cotranslocations using RM were performed as described previously (26). The reactions were performed at 25 °C for 30 min in a final volume of 20 μl containing 10 μl of rabbit reticulocyte lysate, 0.5 μl of ribonuclease inhibitor (40 units/μl), 0.4 μl of a 1 mmol/liter amino acid mixture without methionine and cysteine, 1.6 μl of [^{35}S]methionine (3.7×10^{13} Bq (1000 Ci/mmol)) at 370 MBq (10 mCi/ml), 1.6 μl of [^{35}S]cysteine (3.7×10^{13} Bq (1000 Ci/mmol)) at 370 MBq (10 mCi/ml), and 1 μg of capped mRNA with or without 1 eq of RM.

The translation products were chilled on ice and mixed with 30 μl of buffer A containing 110 mmol/liter potassium acetate, 2.5 mmol/liter magnesium acetate, and 25 mmol/liter potassium-HEPES (pH 7.4). For deglycosylation, 1 μl of Endo H (1 milliunits/μl) and 1 μl of 5% CHAPS were added to a 10-μl aliquot of the diluted translation products and incubated for 1 h at 37 °C. Before being subjected to SDS-PAGE analysis, the samples were precipitated with 2 volumes of saturated $(NH_4)_2SO_4$, washed with 5% trichloroacetic acid, and redissolved in 10 μl of SDS-PAGE sample buffer.

Expression of HPC4-tagged VKOR in Insect Cells and Protease Digestion of VKOR Microsomes—Full-length VKOR molecules with a HPC4 tag at either the N or C termini were expressed in insect cells. Microsomes from cells expressing HPC4-VKOR or VKOR-HPC4 were prepared as described (27). Microsome protein concentrations were adjusted to 10 mg/ml. For protease digestion 2 μl of proteinase K (1 mg/ml) was added to a 10-μl aliquot of freshly prepared microsome in the presence or absence of 0.5% CHAPS as the final concentration. The reactions were carried out on ice for 2 h and terminated by adding phenylmethylsulfonyl fluoride to a final concentration of 3 mmol/liter. After protease digestion, the microsomes were washed 3 times with buffer A containing 3 mmol/liter phenylmethylsulfonyl fluoride, and the pellets were dissolved in SDS sample buffer and subjected to SDS-PAGE analysis.

NuPAGE and Western Blot Analysis—NuPAGE analysis was performed according to the manufacturer's instructions under reducing conditions using 1× MES running buffer (50 mM MES, 50 mM Tris, 1 mM EDTA, and 0.1% SDS (pH 7.3). Samples from the *in vitro* translation were subjected to 4–12% gradient NuPAGE. After electrophoresis the proteins were transferred to a PVDF membrane (0.2 μm), and autoradiography was performed (Amersham Biosciences Storm 840 PhosphorImager). Samples of recombinant HPC4-taged VKOR microsome and protease-digested microsome were subjected to 12% NuPAGE and transferred to a PVDF membrane as above. Protein bands were probed with anti-HPC4 monoclonal antibody followed by a horseradish peroxidase-conjugated secondary antibody, and the protein bands were detected using the enhanced chemiluminescence Western blot reagents.

TABLE I

Prediction of membrane topology of VKOR by different membrane topology prediction programs

Membrane topology of VKOR was predicted by different predication programs using the default parameters. The combined four candidate TM domains are listed. Numbers under the TM correspond to the amino acid residue of VKOR.

Programs	TM no.	C terminus	TM1	TM2	TM3	TM4
PHD	2	In[a]		85–109 (1.0)[b]		119–143 (0.87)
TMHMM 2.0	3	In	10–29 (1.0)		101–123 (0.90)	127–149 (0.93)
TopPred 2	3	In	9–29 (0.65)	78–98 (0.67)	109–129 (1.0)	
TMPred	3	In	9–29 (0.81)	75–97 (0.57)	101–129 (1.0)	
DAS	3		12–27	83–96	102–146	
SOSUI	3		11–31 (primary)	75–97 (secondary)		116–138 (primary)
MEMSAT	4	In	13–29 (0.76)	81–97 (0.60)	104–124 (1.0)	131–148 (0.68)

[a] In, cytoplasmic location of ER.
[b] Numbers in the parentheses are the probability of the predicted TM segment servers as the stop-transfer sequence.

RESULTS

Prediction of the Membrane Topology of VKOR by Different Computer-prediction Algorithms—The membrane topology of VKOR was predicted using seven different topology prediction programs (us.expasy.org/tools/#ptm) with the default parameters. The results are listed in Table I. As can be seen, five of the seven programs predict three TM domains in VKOR, PHD predicts two, and MEMSAT predicts four TM domains. The five programs that predict the location of the C terminus all agree that the C terminus of VKOR is located in the cytoplasm. All programs except PHD predict that the first TM domain comprises residues 10 through 29. The remaining TM domain predictions are somewhat variable for the different prediction programs. The combined candidate TM domains in VKOR predicted by all the programs used are 10–29, 75–97, 101–123, and 127–149. It has been reported that the reliability of topology predictions is greatly increased if different topology prediction methods give the same prediction (19, 20). Therefore, it is likely that VKOR has three TM domains with the C terminus located in the cytoplasm and N terminus located in the ER lumen. Fig. 1 shows the membrane topology prediction and the probability profile of VKOR by the most commonly used prediction program TMHMM. It predicts that VKOR has 3 TM domains, 10–29, 101–123, and 127–149, with the orientation of $N_{exoplasmic}/C_{cytoplasmic}$. One candidate TM domain (75–97), predicted by other programs but not by TMHMM, is indicated in Fig. 1.

VKOR Fusions with the N-Linked Glycosylation Reporter Tag—The glycosylation mapping technique (28) was used in this study to experimentally determine the membrane topology of VKOR. A conserved *N*-linked glycosylation acceptor site (NST) was introduced at either the N or C termini of the full-length VKOR or various VKOR truncations. According to the predicted membrane topology of VKOR, only nine amino acid residues precede the first candidate TM domain. Moreover, if the last predicted TM domain ends at residue149, as predicted by TMHMM and MEMSAT, only 13 C-terminal amino acid residues protrude from the membrane. It has been reported that half-maximal glycosylation occurs when the acceptor Asn is 10~14 residues away from the membrane (28, 29). Therefore, we added flexible amino acid linkers to extend the Asn glycosylation acceptor site away from the membrane. The amino acid sequence of the N-terminal NST tag is MGG**NST**GGSGGSGGSG, and the C-terminal NST tag sequence is SGGSGGS**NST**GGSG. The above extended NST tags were joined to the N or C terminus of full-length VKOR and to all of the VKOR truncations except when otherwise stated. In addition, we fused a dimer C-terminal NST tag at the C terminus of full-length VKOR (VKOR-NST_2). To examine whether the predicted TM region of 75–97 or 101–123 is the authentic TM domain, we deleted the predicted TM region of 75–97 in the fusion of 1–130-NST (1–75/98–130-NST). In addition, we fused a NST glycosylation tag without the flexible linker (**NST**-GGGS) immediately to the C terminus of VKOR truncation 1–130. All the constructs used are shown in Fig. 2.

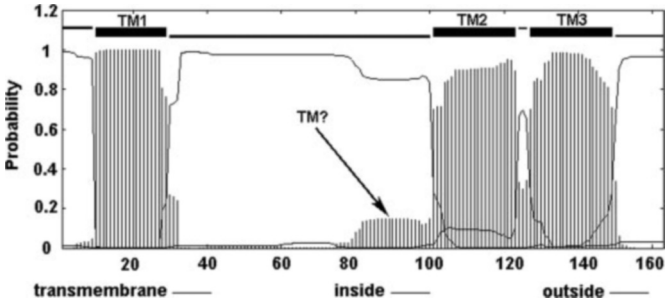

FIG. 1. **TMHMM topology prediction and probability profile for VKOR.** The *top line* shows the predicted topology with the predicted TM helices. The *thin black* and *gray curves* show the posterior probabilities for the inside and outside loops, respectively. The *striped* profile shows the probability for TM helix. Several other algorithms were also used for VKOR topology prediction as described under "Results," a potential TM region predicted by other programs is indicated as *TM?* in this figure.

In Vitro Translation/Cotranslocation of the NST-tagged Full-length VKOR Fusions—Fig. 3 shows the autoradiograph of the *in vitro* translation of the full-length VKOR and NST-tagged full-length VKOR in the presence and absence of RM. As can be seen, N-terminal tagged VKOR, NST-VKOR, is glycosylated in the presence of RM, and the glycosylation product is sensitive to Endo H treatment, which specifically cleaves *N*-linked core sugars. This result indicates that the N terminus of VKOR is located in the ER lumen. In contrast, neither C-terminal tagged VKOR (VKOR-NST or VKOR-NST_2) is glycosylated (Fig. 3), suggesting that the C terminus of VKOR is located in the cytoplasm. These results together suggest that VKOR is a type III membrane protein with the orientation of $N_{exoplasmic}/C_{cytoplasmic}$, and it has an odd number of TM domains. This agrees with the topology model predicted by five of the seven topology prediction programs listed in Table I. In addition, neither of the two natural potential glycosylation sites in the VKOR sequence, Asn-77 and Asn-142, is glycosylated; this is consistent with the prediction of TMHMM, which indicates that Asn-77 is located on the cytoplasm side of the membrane, and Asn-142 is located within the membrane.

Determination of the Signal-anchor Potential of the Predicted TM Domain by in Vitro Translation/Cotranslocation—According to the computer-generated predictions, there are four potential TM segments in VKOR sequence. Therefore, C-terminal truncations of VKOR were made after each of the predicted potential TM segments. The *N*-linked glycosylation reporter tag was fused to either the N terminus or the C terminus of these truncations (Fig. 2). Fig. 4 shows the *in vitro* translation/cotranslocation results obtained from these NST-tagged VKOR truncations in the presence and absence of RM and the pro-

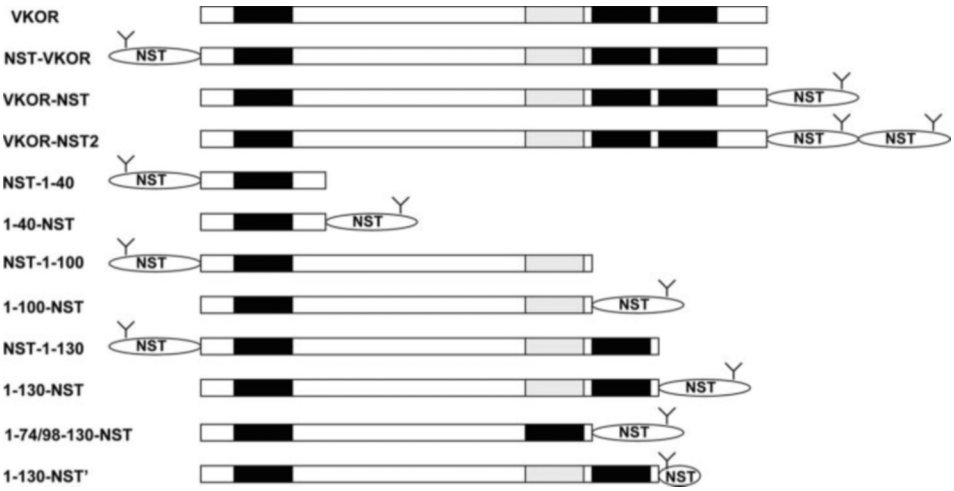

FIG. 2. **Schematic representation of the NST tagged full-length VKOR and VKOR truncation constructs.** The *solid bars* indicate the TM segments predicted by program TMHMM, and the *gray bars* indicate the TM segments predicted by other programs listed in Table I. *Y* indicates the *N*-linked glycosylation acceptor sites.

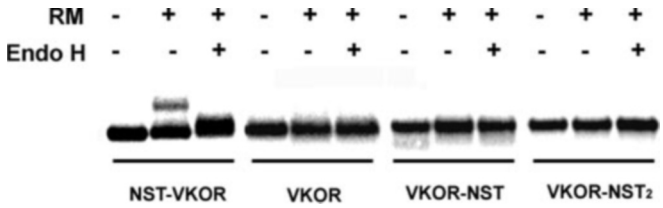

FIG. 3. **Localization of the N and C termini of the VKOR in ER membrane by *in vitro* translation/cotranslocation.** *In vitro* translation/translocation of full-length VKOR and NST-tagged VKOR were performed in the presence (+) and absence (−) of RM. Endo H treatment was performed in the presence of 0.5% CHAPS.

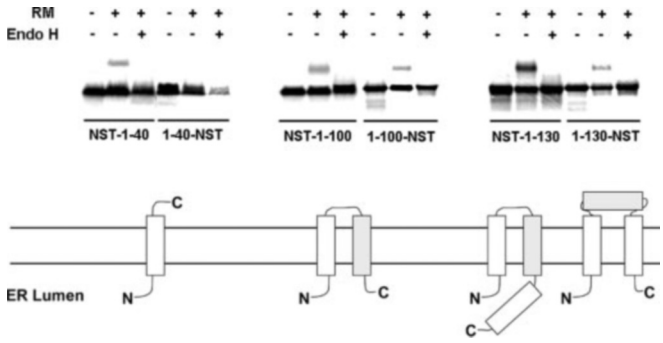

FIG. 4. **Analysis of the individual predicted TM segments.** *In vitro* translation/translocation of NST-tagged VKOR truncations were performed in the presence (+) and absence (−) of RM. Endo H treatment was performed in the presence of 0.5% CHAPS. Possible orientation of each truncation was elucidated on the *bottom*.

posed topological orientation. As can be seen, NST-1–40 was glycosylated, but 1–40-NST was not, indicating that the first predicted TM segment, 10–29, can function as a reverse signal-anchor sequence, characteristic of type III membrane protein. Both fusions of NST-1–100 and 1–100-NST were glycosylated, indicating that both the N and C termini are located in the ER lumen with the hairpin structure. Together with the result of fusion 1–40, this result suggests that the second predicted TM domain, 75–97, can function as a signal-anchor sequence. However, both fusions of NST-1–130 and 1–130-NST, which has one more predicted TM domain than fusion 1–100, are also glycosylated, indicating that they have the same topological orientation as fusion 1–100. This result raises the question of whether the additional predicted TM domain of 101–123 in the fusion of 1–130 functions as the signal anchor sequence.

Predicted TM Region of 101–123 Functions as a Genuine TM Domain—To examine whether the predicted TM region of 101–123 functions as a genuine TM domain, we deleted the potential TM region of 75–97 in the fusion of 1–130-NST (1–75/98–130-NST) (Fig. 2). As shown in Fig. 5*A*, the C-terminal glycosylation tag can be glycosylated in the presence of RM, indicating that the C terminus is located in the lumen of ER. Together with the result of fusion 1–40, this result suggests that the predicted TM region of 101–123 functions as a genuine TM domain in the fusion 1–75/98–130-NST.

In a further attempt to determine which of the potential TM domains, 75–97 or 101–123, functions as the genuine TM domain in the VKOR truncation 1–130, a glycosylation reporter tag with the sequence of **NST**GGGS was fused to the C terminus of VKOR-1–130 (1–130-NST′). This places the Asn glycosylation acceptor site immediately after the predicted TM segment 101–123. According to the "minimum glycosylation distance" rule (28, 29), this tag should not be glycosylated if 101–123 functions as the stop-transfer sequence in this construct. On the other hand, if 75–97 serves as a TM domain, this tag should be glycosylated since there is enough extension sequence between the Asn acceptor site and the TM segment. As shown in Fig. 5*B*, no glycosylated product was detected in the presence of RM. This result suggests that the predicted TM segment 101–123 is the functional TM domain in the VKOR truncation 1–130, but 75–97 does not.

Independent Determination of the Topological Orientation of N and C Termini of VKOR in Vivo—To determine the topological orientation of the N and C termini of VKOR *in vivo*, we constructed two full-length recombinant VKOR molecules tagged with a HPC4 epitope at either end, HPC4-VKOR and VKOR-HPC4. Both VKOR constructs expressed in insect (Sf9) cells displayed kinetic parameters characteristic of the non-tagged VKOR, indicating correct folding of the recombinant-tagged enzymes (data not shown). Freshly prepared microsomes from the Sf9 cells expressing these constructs were subjected to proteinase K digestion in the presence or absence of 0.5% CHAPS and subjected to NuPAGE analysis. The protein bands were transferred to a PVDF membrane and probed with the anti-HPC4 antibody and visualized by enhanced chemiluminescence reagents.

As shown in Fig. 6, proteinase K digestion of the HPC4-VKOR revealed a protected fragment (indicated by an *arrow*), that was rendered sensitive to proteinase K digestion by prior

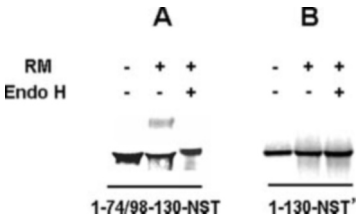

FIG. 5. **Evidence that the predicted TM domain 101–123 is the third transmembrane segment.** *A*, the second predicted TM region of 75–97 was deleted in the VKOR truncation fusion of 1–130-NST (1–74/98–130-NST). *In vitro* translation/translocation was performed in the presence (+) and absence (−) of RM. Endo H treatment was performed in the presence of 0.5% CHAPS. *B*, a NST glycosylation tag was directly fused to the C terminus of VKOR truncation 1–130, which places the Asn glycosylation site immediately after the predicted TM segment of 101–123 (1–130-NST′). *In vitro* translation/co-translocation of 1–130-NST′ was performed in the presence (+) and absence (−) of RM. Endo H treatment was performed in the presence of 0.5% CHAPS.

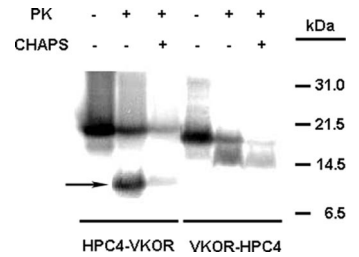

FIG. 6. **Localization of the N and C termini of the VKOR *in vivo*.** Freshly prepared intact microsomes from insect cells expressing HPC4-VKOR or VKOR-HPC4 were subjected to proteinase K (*PK*) digestion in the presence (+) and absence (−) of 0.5% CHAPS. Samples were fractionated by reducing SDS-PAGE, and protein bands were transferred to PVDF membrane for Western blot. The anti-HPC4 antibody was used as the secondary antibody for the Western blot analysis. Microsome membrane protected band was marked by an *arrow*.

CHAPS treatment. This indicates the lumenal location of the HPC4 tag and, therefore, the N terminus of the VKOR. In contrast, no protease-protected fragment was observed when microsomes expressing VKOR-HPC4 were treated with proteinase K. This is consistent with the cytoplasmic location of the HPC4 tag and, therefore, the C terminus of the VKOR. These data together suggest that VKOR has a topological orientation of $N_{exoplasmic}/C_{cytoplasmic}$ that is in agreement with the above *in vitro* translation/cotranslocation results.

DISCUSSION

Determining the membrane topology, *i.e.* specification of its TM segments and their cytoplasmic/exoplasmic orientation relative to the membrane, is an important first step in understanding the function of any integral membrane enzyme. Rost *et al.* (17) suggested that there are three TM domains in VKORC1, whereas Li *et al.* (16) suggested that there may between one-to-three TM domains depending on the programs used for the membrane topology prediction. Recently, Goodstadt *et al.* (30) suggested that rather than the one-to-three TM domain model, there are four TM domains in VKOR. All of the previous predictions were based upon topology prediction programs; therefore, in this study we attempt to resolve this issue experimentally.

First, to identify the most likely TM domain candidates, we used seven different computer programs to predict the membrane topology of VKOR. Five of seven programs agree that VKOR has three TM domains with the N terminus located in the lumen and C terminus located in the cytoplasm; however, the programs that predict three TM domains do not agree on their location. One program predicts two TM domains in VKOR, whereas another predicts four. We designed experiments to determine which of the four potential TM domains are real. To accomplish this we employed the *in vitro* glycosylation mapping assay (28, 29).

In the presence of canine rough microsomes, full-length VKOR as well as VKOR truncations with N-terminal NST tags are glycosylated by the *in vitro* translation/cotranslocation system. These results strongly suggest that VKOR is a type III membrane protein with its N terminus in the ER lumen. This interpretation was confirmed by the observation that an HPC4 tag at the N terminus of full-length VKOR in intact insect microsomes was protected from protease digestion unless the membrane was first solubilized with CHAPS. In addition, the result with NST-1–40 indicates that the first predicted TM segment (10–29) is authentic. Thus, the location of the N terminus of VKOR and the position of the first TM domain is established.

The authenticity of the next two predicted TM domains, residues 75–97 and 101–123, is less clear. Both the N- and C-terminal NST tags of VKOR-1–100 and 1–130 are glycosylated in the *in vitro* canine rough microsome system. This result indicates that the C termini of both truncations are located in the lumen of the ER (Fig. 4). Because the first predicted TM domain (10–29) is authentic, the implication of these results is that the second predicted TM domain (75–97) is real in VKOR-1–100. Furthermore, based on these results there is no reason to assume that it is not also a real TM domain in VKOR-1–130. However, according to the prediction programs, residues 101–123 have a higher probability of functioning as a TM domain than do residues 75–97 (Table I). Therefore we tested whether 101–123 functions *in vitro* as a TM domain by deleting residues 75–98 from VKOR-1–130-NST (1–74/98–130-NST). In this construct the C-terminal NST tag is still glycosylated in the presence of RM (Fig. 5*A*); this result indicates that the third predicted TM domain (101–123) can also function as an authentic TM domain. Together, these results suggest that *in vitro* the second and the third predicted TM domain both can function as TM domains. Which, then, is functional in VKOR-1–130 and the intact protein?

As mentioned above, the topology prediction programs indicate that residues 101–123 have a higher probability of being a TM domain than do residues 75–97. To further examine this question experimentally, we made a NST-tagged fusion of VKOR-1–130 that did not have a flexible linker; that is, the Asn glycosylation acceptor site was placed immediately after residue 130 (1–130-NST′). If the third predicted TM domain is a functional TM domain, then this fusion should not be glycosylated because of insufficient distance between the Asn acceptor and TM segment (4, 5). As shown in Fig. 5*B*, no glycosylation product was observed in the presence of RM, suggesting that the third predicted TM domain is real in VKOR-1–130-NST′. This result is again consistent with the notion that residues 101–123 and not 75–97 constitute the functional TM domain in VKOR-1–130 and in the intact protein.

The result of *in vitro* translation/co-translocation of NST tagged full-length VKOR (Fig. 3) demonstrates that the N-terminal NST tag can be glycosylated, but the C-terminal tag cannot. Despite these results, it is still formally possible that the C terminus resides in the lumen and that the failure to glycosylate the NST tag at the C terminus of full-length VKOR is because of its close proximity to the membrane or to low glycosylation efficiency (31). Therefore, we fused a dimer NST tag to the C terminus of full-length VKOR (VKOR-NST_2). If the C terminus really was luminal, then the additional tag should extend the Asn acceptor site away from the membrane to allow glycosylation. However, even with this construct, no glycosylation was observed in the presence of RM (Fig. 3). Therefore, we conclude that the C terminus of intact VKOR is exposed on the

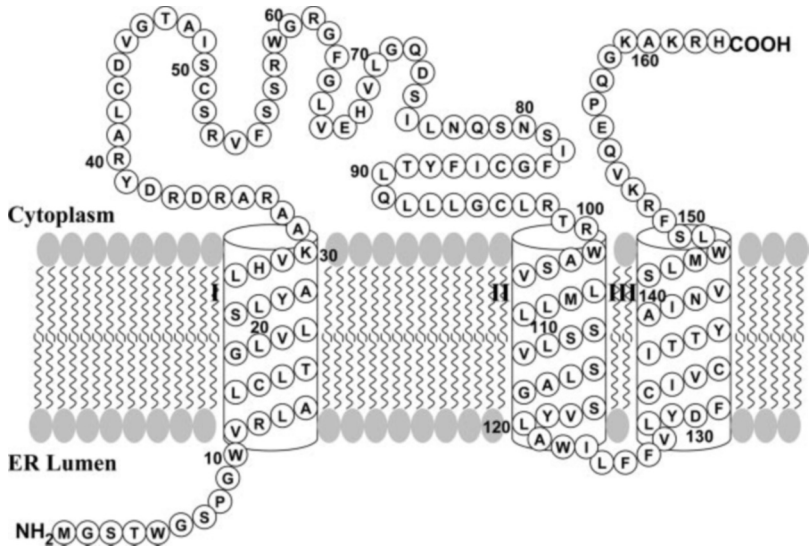

FIG. 7. **Proposed membrane topology of VKOR.**

cytoplasmic side of the ER. The fourth *predicted* (the third functional) TM domain (127–149) functions as a genuine TM domain in intact VKOR. Further evidence that the C terminus of VKOR resides in the cytoplasm was provided by experiments where an antibody tag (HPC4) was added to the C terminus of full-length VKOR (VKOR-HPC4). Intact microsomes were prepared from insect cells expressing VKOR-HPC4 and were treated with proteinase K. This tag was destroyed by proteinase treatment, whereas a lumenal N-terminal tag was protected (Fig. 6).

Altogether, our data suggest that there are three TM domains (10–29, 101–123, and 127–149) in VKOR and that the N terminus of VKOR is located in the lumen of the ER, whereas the C terminus is located in the cytoplasm (Fig. 7). Our results agree with the membrane topology predicted by most of the computer prediction programs. The N-terminal domain of VKOR, like many type III membrane proteins, is relatively short, which facilitates its transfer into the lumen. Only 12 of 163 amino acids are luminal, whereas 85 residues are located in the cytoplasm, and 66 residues are buried in the ER membrane. Thus, it seems unlikely that the active site residues reside in the lumen of ER. Moreover, it seems likely that the active site is either in the cytoplasm or the membrane itself.

There is a large cytoplasmic loop that includes hydrophilic and hydrophobic regions and also contains two (Cys-43 and Cys-51) of the four absolutely conserved cysteines of VKOR. Goodstadt and Ponting (30) proposed that these two cysteines were part of the active site of VKOR. However, in their four TM domain model, the loop containing Cys-43 and Cys-51 is in the lumen of the ER, whereas in our experimental model this loop is cytoplasmic. Although the activity of the vitamin K-dependent carboxylase resides in the lumen of the ER, it is possible that the active site of VKOR could be in the cytoplasm or even within the membrane as vitamin K is very hydrophobic.

Goodstadt and Ponting (30) proposed that a C*XX*C motif was at least part of the active site of VKOR. The C*XX*C motif is the active site in a number of thioredoxin and protein disulfide isomerase enzymes (32). In keeping with this idea, there is extensive literature detailing the importance of cysteines in the activity of VKOR (11, 12, 14, 33–38) and that the active site cysteines reside in a hydrophobic environment (33). Recently, Wajih *et al.* (39) reported that mutation of Cys-132 or Cys-135 (the C*XX*C motif in VKOR) to alanine abolished VKOR activity. This is consistent with the C*XX*C motif serving as the redox center for VKOR. According to our results, the conserved C*XX*C motif is located within the third TM domain and is buried in the membrane.

In conclusion, our results suggest that VKOR is a type III membrane protein with three TM domains. The majority of the molecule is located on the cytoplasm side of the ER membrane. The topology model provides a clear picture of the distribution of the amino acid residues of VKOR around the ER membrane, which can be used as the guide for its function study. The observation that a likely active site motif is within a TM segment may provide an explanation for the difficulties encountered in the purification of VKOR (10). That is, its efficient solubilization may lead to loss of activity.

Acknowledgments—We thank Dr. Tao Li for helpful discussions. We also thank Tianli Zheng for excellent technical assistance.

REFERENCES

1. Presnell, S. R., and Stafford, D. W. (2002) *Thromb. Haemostasis* **87,** 937–946
2. Price, P. A. (1988) *Annu. Rev. Nutr.* **8,** 565–583
3. Manfioletti, G., Brancolini, C., Avanzi, G., and Schneider, C. (1993) *Mol. Cell. Biol.* **13,** 4976–4985
4. Furie, B., Bouchard, B. A., and Furie, B. C. (1999) *Blood* **93,** 1798–1808
5. Saxena, S. P., Israels, E. D., and Israels, L. G. (2001) *Apoptosis* **6,** 57–68
6. Bell, R. G., and Matschiner, J. T. (1970) *Arch. Biochem. Biophys.* **141,** 473–476
7. Mukharji, I., and Silverman, R. B. (1985) *Proc. Natl. Acad. Sci. U. S. A.* **82,** 2713–2717
8. Lee, J. J., Principe, L. M., and Fasco, M. J. (1985) *Biochemistry* **24,** 7063–7070
9. Wallin, R., and Guenthner, T. M. (1997) *Methods Enzymol.* **282,** 395–408
10. Cain, D., Hutson, S. M., and Wallin, R. (1997) *J. Biol. Chem.* **272,** 29068–29075
11. Begent, L. A., Hill, A. P., Steventon, G. B., Hutt, A. J., Pallister, C. J., and Cowell, D. C. (2001) *J. Pharm. Pharmacol.* **53,** 481–486
12. Silverman, R. B., and Nandi, D. L. (1988) *Biochem. Biophys. Res. Commun.* **155,** 1248–1254
13. Preusch, P. C. (1992) *FEBS Lett.* **305,** 257–259
14. Thijssen, H. H., Janssen, Y. P., and Vervoort, L. T. (1994) *Biochem. J.* **297,** 277–280
15. Wallin, R., Hutson, S. M., Cain, D., Sweatt, A., and Sane, D. C. (2001) *FASEB J.* **15,** 2542–2544
16. Li, T., Chang, C. Y., Jin, D. Y., Lin, P. J., Khvorova, A., and Stafford, D. W. (2004) *Nature* **427,** 541–544
17. Rost, S., Fregin, A., Ivaskevicius, V., Conzelmann, E., Hortnagel, K., Pelz, H. J., Lappegard, K., Seifried, E., Scharrer, I., Tuddenham, E. G., Muller, C. R., Strom, T. M., and Oldenburg, J. (2004) *Nature* **427,** 537–541
18. Moller, S., Croning, M. D., and Apweiler, R. (2001) *Bioinformatics* **17,** 646–653
19. Nilsson, J., Persson, B., and von Heijne, G. (2000) *FEBS Lett.* **486,** 267–269
20. Melen, K., Krogh, A., and von Heijne, G. (2003) *J. Mol. Biol.* **327,** 735–744
21. Taylor, P. D., Attwood, T. K., and Flower, D. R. (2003) *Nucleic Acids Res.* **31,** 3698–3700
22. Kim, H., Melen, K., and von Heijne, G. (2003) *J. Biol. Chem.* **278,** 10208–10213
23. Goder, V., and Spiess, M. (2001) *FEBS Lett.* **504,** 87–93
24. Walter, P., and Blobel, G. (1983) *Methods Enzymol.* **96,** 84–93
25. Stearns, D. J., Kurosawa, S., Sims, P. J., Esmon, N. L., and Esmon, C. T. (1988) *J. Biol. Chem.* **263,** 826–832
26. Tie, J., Wu, S. M., Jin, D., Nicchitta, C. V., and Stafford, D. W. (2000) *Blood* **96,** 973–978
27. Mutucumarana, V. P., Stafford, D. W., Stanley, T. B., Jin, D. Y., Solera, J., Brenner, B., Azerad, R., and Wu, S. M. (2000) *J. Biol. Chem.* **275,** 32572–32577
28. Nilsson, I. M., and von Heijne, G. (1993) *J. Biol. Chem.* **268,** 5798–5801
29. Nilsson, I., Saaf, A., Whitley, P., Gafvelin, G., Waller, C., and von Heijne, G.

(1998) *J. Mol. Biol.* **284,** 1165–1175
30. Goodstadt, L., and Ponting, C. P. (2004) *Trends Biochem. Sci.* **29,** 289–292
31. Gavel, Y., and von Heijne, G. (1990) *Protein Eng.* **3,** 433–442
32. Gromer, S., Urig, S., and Becker, K. (2004) *Med. Res. Rev.* **24,** 40–89
33. Wallin, R., Sane, D. C., and Hutson, S. M. (2002) *Thromb. Res.* **108,** 221–226
34. Soute, B. A., Groenen-van Dooren, M. M., Holmgren, A., Lundstrom, J., and Vermeer, C. (1992) *Biochem. J.* **281,** 255–259
35. Preusch, P. C., and Smalley, D. M. (1990) *Free Radic. Res. Commun.* **8,** 401–415
36. Wallin, R., Patrick, S. D., and Martin, L. F. (1987) *Int. J. Biochem.* **19,** 1063–1068
37. Suttie, J. W., and Preusch, P. C. (1986) *Haemostasis* **16,** 193–215
38. Lee, J. J., and Fasco, M. J. (1984) *Biochemistry* **23,** 2246–2252
39. Wajih, N., Sane, D. C., Hutson, S. M., and Wallin, R. (2005) *J. Biol. Chem.* **280,** 10540–10547